ELSEVIER

Ceramics International 28 (2002) 651–655

CERAMICS INTERNATIONAL

www.elsevier.com/locate/ceramint

Effect of chromium substitutions on some properties of NiZn ferrites

A.M. El-Sayed*

Inorganic Chemistry Department, National Research Centre, Tahrir Street, Dokki, Cairo 12622, Egypt

Received 12 June 2001; received in revised form 16 July 2001; accepted 6 November 2001

Abstract

Compositions having the general formula $Ni_{0.6}Zn_{0.4}Cr_tFe_{2-t}O_4$ with $t = 0.00$, 0.05, 0.10, 0.15, 0.20 and 0.25 were prepared by the usual ceramic processing from high purity oxides. The samples were sintered at 1250 °C in static air atmosphere. X-ray diffraction and IR absorption spectra were used for analysing the composition. Lattice parameter, true density, bulk density, porosity and shrinkage were measured for the samples. A scanning electron microscope investigation was also carried out. It is observed that all samples have a single phase with spinel cubic structure. Lattice parameter, true density, bulk density are found to increase with increasing Cr concentration, whereas both porosity, shrinkage and grain size showed a decreasing trend with the Cr content.

Keywords: A. Sintering; B. Microstructure; NiZnCr ferrites; Preparation

1. Introduction

NiZn ferrites have been commercially used for many years as high-frequency ferrites for radio frequency coil, transformer cores and rod antennas [1]. There is a specialized application of NiZn ferrites requiring low porosity and controlled microstructure in the magnetic cores of read write heads for high-speed digital tape or disk recording [2]. Polycrystalline ferrites are a complex system composed of crystallites, grain boundaries and pores. The magnetic properties of these ferrites are determined by chemical composition, porosity, grain size etc. [3]. The substitution of paramagnetic or diamagnetic ions in pure ferrites results in modification of their structural, electrical and magnetic properties [4]. Rezlescu and Rezlescu [5] reported the influence of additives (Ca^{2+}, Na^{+}, Zr^{4+}, Li^{+}, etc.) on the properties of Ni–Zn ferrites. They observed that addition of Li^{+} enhances the intial permeability. Masker et al. [6] have studied the effect of addition of Ti^{4+} on the wall permeability in NiZn ferrites and observed the permeability tends to decrease with the addtion of Ti^{4+}. The aim of the present work is to study the effect of successive increased substitution of Cr^{3+} ions in NiZn ferrite on the ferrite structure, density, porosity, shrinkage and grain size.

2. Experimental

In the present investigation samples having the composition $Ni_{0.6}Zn_{0.4}Cr_tFe_{2-t}O_4$ ($t = 0.00$, 0.05, 0.10, 0.15, 0.20 and 0.25) were studied. The starting materials were AR grade ZnO, NiO, Cr_2O_3 and Fe_2O_3. A small amount of Bi_2O_3 (0.005 wt.%) was added as fluxing agent. Suitable proportions of these materials were dry ground into fine powder and then mixed thoroughly in presence of distilled water to improve the homogeneity using a Retsch ball mixer. The resulting mixture was calcined in air for 4 h at 900 °C. Then the calcined product was well ground again and pellets of 1.25 cm diameter and 0.27 cm thickness were prepared by applying a pressure of 5 ton/cm^2, which were sintered in air for 4 h at 1250 °C and left to cool inside the electric furnace. X-ray diffraction studies were carried out on fine powder of the finally sintered samples with Philips PW 1390 X-ray diffractomter using cobalt target and iron filter. Infrared spectroscopic analysis using KBr pellets was carried out with a FTIR 300E Fourier transform

* Fax: +20-2-337-0931.

0272-8842/02/$22.00
PII: S0272-8842(02)00022-6

infrared spectrometer (Jasco Japan). Bulk density and apparent porosity of the prepared samples were determined as described in British standard methods of testing refractory materials [7]. The percentage change in the diameter of samples before and after sintering was determined. The scanning electron microscope investigation was carried out on a fresh fracture surface. The fracture surface was coated with a thin film of evaporated gold, using a S150 A sputter coater (UK). Scanning electron micrographs were obtained using a JSM-T20 scanning microscope, (Jeol Japan).

3. Results and discussion

In Fig. 1 the X-ray diffraction patterns of the prepared ferrite samples are shown. All samples showed single phase formation. The presence of the peaks corresponding to the planes (111), (220), (311), (222), (440), (422), (511), (440), (620) and (533) in the patterns of the samples confirms the formation of spinel cubic structure. The patterns show also a slight shifting in peaks position towards lower *d*-spacing values with increasing Cr content in the ferrites. The *d*-spacings for the recorded peaks were calculated according to Bragg's law. The values of the calculated lattice constant for various concentration of chromium are given in Table 1. It is shown that the variation of lattice constant with rise in concentration of chromium is linear (Fig. 2). The lattice constant slightly decreases with increase in the amount of Cr content. In chromium-doped ferrites, the Cr ions are known to have strong site preference of B sites [8] leads to the replacement of Fe^{3+} ions at octahedral sites. The variation of lattice constant with increasing Cr content can be explained on the basis of ionic radii of the impurity ions. If the radius of the impurity ion is smaller than the displaced ion, the lattice shrinks and the lattice constant decreases. The reverse will hold if a bigger impurity ion replaces a metal ion of the regular lattice. Since there is a difference between the ionic radii of Cr^{3+} (0.63 Å) and Fe^{3+} (0.64 Å) ions [9], the lattice constant is expected to decrease with increasing Cr content. This behaviour is in agreement with the observation noted by Rao et al. [10] on Cr doped MnZn ferrites. Another observation is that, with increasing Cr concentration in the ferrite composition (Fig. 1), the peaks intensity in the patterns are shown to decrease. This variation can be attributed to the increase of Cr

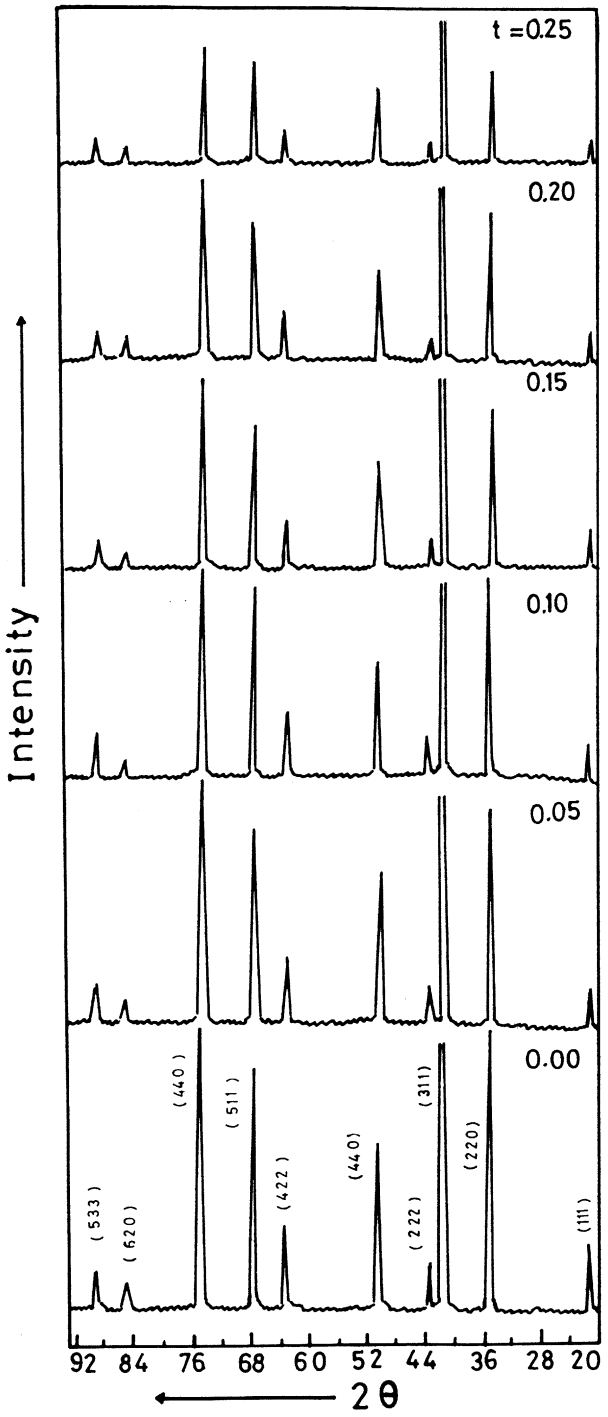

Fig. 1. X-ray diffraction patterns of $Ni_{0.6}$ $Zn_{0.4}Cr_tFe_{2-t}O_4$ sintered at 1250 °C.

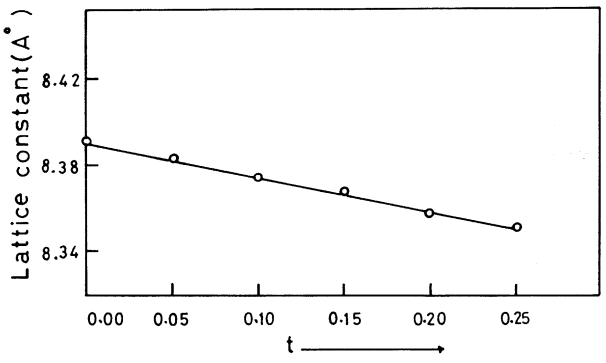

Fig. 2. Variation of lattice constant with Cr content in $Ni_{0.6}Zn_{0.4}$ $Cr_tFe_{2-t}O_4$.

Table 1
The obtained data of $Ni_{0.6}Zn_{0.4}Cr_tFe_{2-t}O_4$

T	Lattice constant Å	ν_2 cm^{-1}	X-ray density (g/cm^3)	Bulk density $(g/cm)^3$	Apparent porosity (%)	Diameter shrinkage (%)
0.00	8.392	399	5.330	5.203	2.38	12.35
0.05	8.382	400	5.344	5.225	2.22	12.75
0.10	8.373	404	5.358	5.248	2.05	13.02
0.15	8.366	409	5.367	5.266	1.87	13.45
0.20	8.357	415	5.380	5.287	1.73	13.75
0.25	8.350	420	5.392	5.300	1.63	13.95

concentration in the ferrite compositions which affects the ferrite crystallinity.

In Fig. 3, the IR spectra of the samples are shown from 200–1400 cm^{-1}. The spectra show two main absorption bands below 1000 cm^{-1} as a common feature of all the ferrites. The bands at 585 cm^{-1} and around 410 cm^{-1} are assigned as ν_1 and ν_2 respectively [11]. The band lower than ν_2 is assigned as ν_3. Also the spectrum shows that no shift occurs in band position at frequency ν_1 by increasing Cr content. Meanwhile, it can be seen that the frequency ν_2 is shifted to higher frequencies with increasing Cr ion concentration in the ferrite (Table 1) and consequently decreasing iron ions. The absorption band ν_1 is caused by the stretching vibration of the tetrahedral metal-oxygen bond, and the absorption band ν_2 is caused by the metal-oxygen vibrations in octahedral sites [12]. Thus, the replacement of Fe ions with Cr ions at octahedral sites [8] which

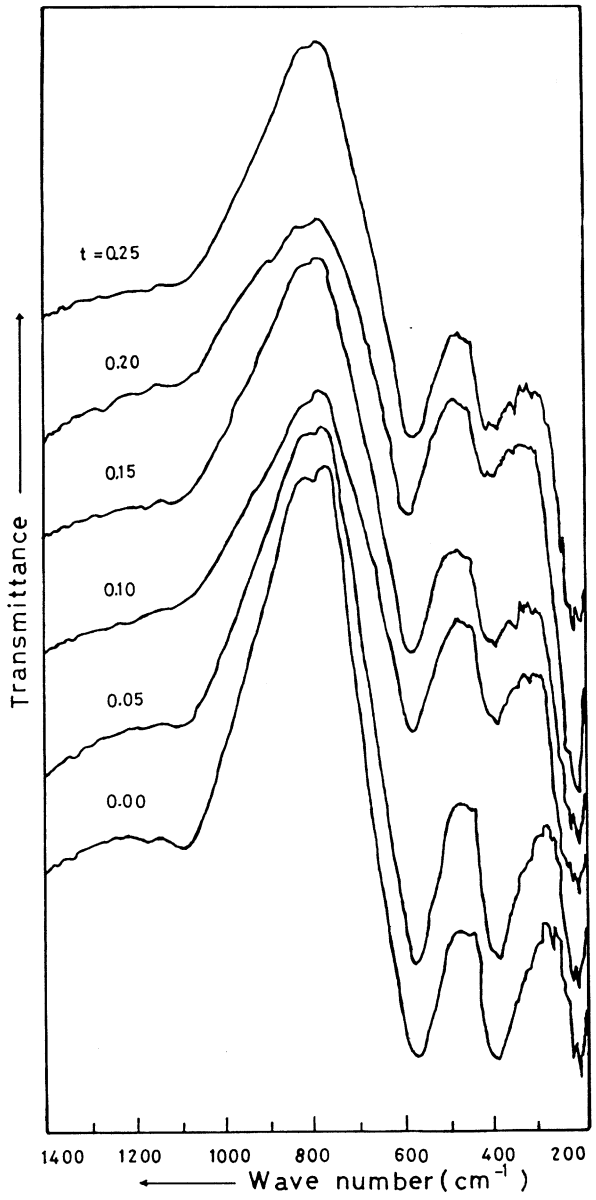

Fig. 3. IR absorption spectra of $Ni_{0.6}Zn_{0.4}Cr_tFe_{2-t}O_4$ sintered at 1250 °C.

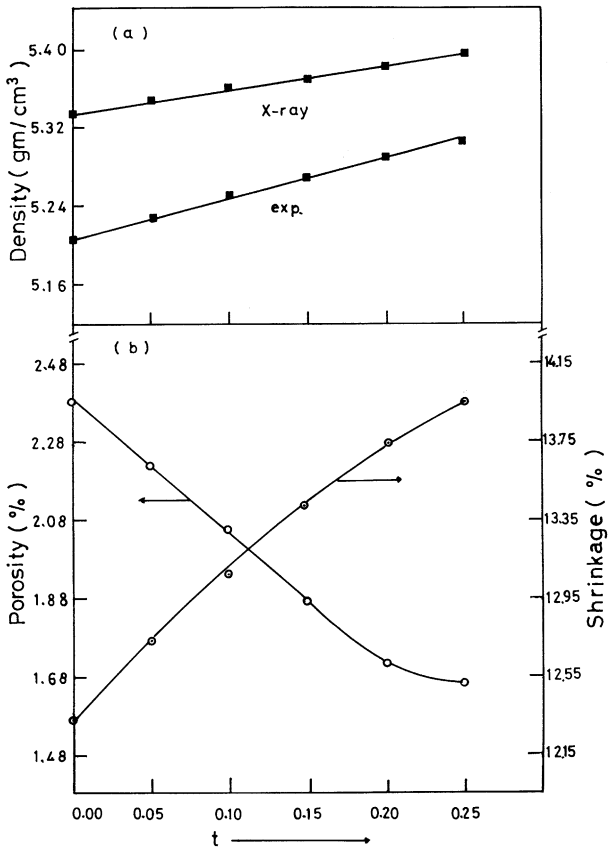

Fig. 4. Variation of (a) X-ray density and bulk density; (b) apparent porosity and diameter shrinkage, with Cr content in $Ni_{0.6}Zn_{0.4}Cr_tFe_{2-t}O_4$.

have smaller ionic radius and lower atomic mass, is the important reason of the observed shift in the band position (ν_2) with increasing Cr content in the ferrite. Also, from IR spectra (Fig. 3) it is noticed that intensity of the absorption band (ν_2) decreases with increasing Cr concentration. It is known that the intensity ratio is a function of the change of dipole moment with the internuclear distance ($d\mu/dr$) [13]. This value represents the contribution of the ionic bond Fe–O in the lattice. So, the observed decrease in the absorption band (ν_2) intensity with increasing Cr content is presumably due to the perturbation occurring in Fe–O bonds by substitution the Cr^{3+} ions. On the other hand, the electronic distribution of Fe–O bonds is greatly affected when a Cr^{3+} ion with ($3d^4 4S^2$) orbitals is introduced in its neighbourhood and this consequently affects ($d\mu/dr$) of the Fe–O bond.

The variation of bulk density (d_{exp}) with Cr concentration, as well as the X-ray density (d_x) variation are represented in Fig. 4a. The X-ray density (true density) of the prepared specimens was calculated from X-ray diffraction patterns [14]. From Fig. 4a it is clearly shown that the bulk density was found to increase with increasing Cr content. The same behaviour was observed with X-ray density. The true densities are higher than the bulk values, this is attributed to the porosity of such prepared samples. The bulk densities of the specimens are found to be more or less within the range (97.6–98.3%) of the corresponding X-ray densities (Table 1).

The effect of Cr substitution on the porosity of the prepared specimens is observed in Fig. 4b. The chromium substitution reduces the porosity thus increasing the density of the sample. Since the increase of bulk density is of order 0.097 g/cm^3 with Cr content while the increase of X-ray density is of order 0.062 g/cm^3, one can expect the porosity to decrease with increasing Cr content. The small difference between d_{exp} and d_x at higher concentration of Cr ($t=0.25$) is due to the decrease in porosity percentage (Table 1). Fig. 4b shows the variation in the percentage shrinkage of the diameter of the discs with Cr content. It is noticed that shrinkage and porosity behave inversely to each other with respect to Cr concentration. The highest shrinkage (13.95%) and the lowest porosity (1.63%) were found for the sample with $t=0.25$.

Scanning electron micrographs of the prepared samples are given in Fig. 5. It can be easily observed that the

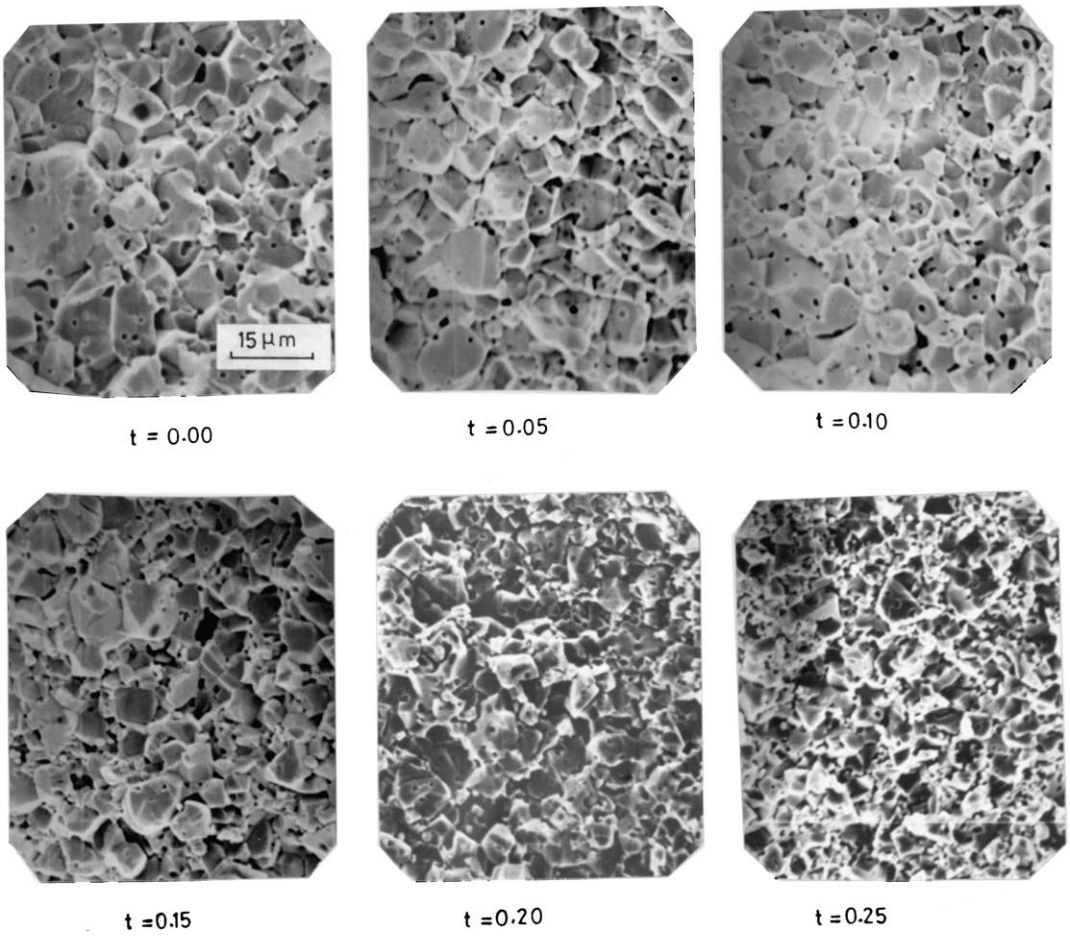

Fig. 5. Scanning electron micrographs of $Ni_{0.6}Zn_{0.4}Cr_tFe_{2-t}O_4$ sintered at 1250 °C.

grain size decreases with increasing Cr concentration in the ferrite. The micrograph of the sample of pure NiZn ferrite ($t=0$) illustrates large grains with some pores at grain boundaries and little fine pores entrapped within the grains. On increasing Cr content the micrographs show a decrease in the ferrite porosity. The increase in Cr content causes lowering in both grain size and values of porosity and the stronger effect is obtained with high Cr content ($t=0.25$). Yan and Johnson [15] concluded that, the dissolution of an oxide dopant with 2+ cation valence in Mn–Zn ferrite does not created excess cation vacancies. Dopants with 3+ cation valence generate little excess cation vacancy concentration in the ferrite lattice. They also attributed the absence of enhanced grain growth for dopant oxides with 2+ or 3+ cation valence to the lake of a significant number of excess cation vacancies in the ferrite lattice. In lithium ferrites, Bandyopahyay and Fulrath [16] observed that, compositions with excess Fe_2O_3 had a microstructure with discontinuous grain growth and pores entrapped within the grains. They also found that, the excess Fe_2O_3 in the ferrite composition results in a higher cation vacancy concentration and lower density. The low cation vacancies can reduce the flux of cation diffusion and hence pore migration will be retarded. As a consequence, it was observed that pores were trapped inside the grains [17]. Thus, the increasing in Cr (3+) concentration which is accompanied by a decrease in Fe_2O_3 content in the ferrite results in a decrease in cation vacancies. The decrease in cation vacancies with increasing Cr content in the prepared specimens may be the reason for the observed decrease in both grain size and porosity values, and the increasing in bulk density. Recently, Sankpal et al. [18] suggested that Cr ions, which tend to decrease the grain size, cause impedance to the domain wall motion in NiZn ferrite and that the higher the concentration of these ions the more the wall motion is impeded.

4. Conclusion

1. The substitutions of Cr ions in $Ni_{0.6}$ $Zn_{0.4}$ Cr_t $Fe_{2-t}O_4$, sintered at 1250 °C in air, lead to formation of ferrites having single phase and cubic spinel structure with decreasing lattice constant.
2. With increasing Cr concentration in the ferrite, a shifting in the IR band position (ν_2) to higher frequencies with a decrease in its IR absorption intensity are observed.
3. The replacement of iron with chromium at octahedral sites in the ferrite presumably leads to a decrease in cation vacancies. This leads to a decrease of both % porosity and grain size whereas the bulk density is observed to increase. The stronger effect is obtained with high Cr content ($t=0.25$).

References

[1] E.E. Riches, in: J. Gordon Cook (Ed.), Ferrites, A Review of Materials and Applications, Mills and Boons, London, 1972, p. 17.
[2] J. Kulikowski, A. Lesiewski, Properties of nickel ferrites for magnetic materials, J. Magn. Magn. Mater. 19 (1980) 117–119.
[3] H. Igarashi, K. Okazaki, Effects of porosity and grain size on the magnetic properties of NiZn ferrite, J. Am. Ceram. Soc. 60 (1977) 51–54.
[4] J.L. Dormann, T. Merceron, M. Nogues, Proc. Int. Cong. on the Applications of the Mössbauer Effect, Jaipur, India, 1981, p. 193.
[5] N. Rezlescu, E. Rezlescu, The influence of iron substitutions by R ions in a nickel zinc ferrite, Solid State Commun. 88 (1993) 139–141.
[6] P.K. Maskar, S.V. Kakatkar, A.M. Sankpal, R.S. Patil, S.S. Suryavanshi, S.R. Sawant, Wall permeability studies on Ti^{4+} doped NiZn ferrite, J. Czech. Phys. 46 (1996) 397–400.
[7] British Standard Institution, Methods of Testing Refractory Materials, 1952, 1902, 21–25.
[8] N.K. Gill, R.K. Puri, Mossbauer study of $Li_{0.5}Fe_{2.5-x}Cr_xO_4$ ferrites, Spectrochimica Acta. 41A (1985) 1005–1008.
[9] R.C. Weast, M.J. Astle Handbook of Chemistry and Physics, CRC Press. Inc., FL, 1981, p. F-175.
[10] K.H. Rao, N.K. Gaur, K. Aggarwal, R.G. Mendiratta, Effect of additives on the properties of zinc-–manganese ferrite, J. Appl. Phys. 53 (1982) 1122–1126.
[11] V.A.M. Brabers, Infrared spectra of cubic and tetragonal manganese ferrites, Phys. Stat. Sol. 33 (1969) 563–572.
[12] R.D. Waldron, Infrared spectra of ferrites, Phys. Rev. 99 (1955) 1727–1735.
[13] S.A. Mazen, M.H. Abdallah, B.A. Sabrah, H.A.M. Hashem, The effect of titanium on some physical properties of $CuFe_2O_4$, Phys. Stat. Sol. (a) 134 (1992) 263–271.
[14] A.M. El-Sayed, Preparation and structural investigations of titanium substituted Li–Zn ferrites, Egypt. J. Chem. 40 (1997) 295–303.
[15] M.F. Yan, D.W. Johnson, Impurity-induced exaggerated grain growth in Mn–Zn ferrites, J. Am. Ceram. Soc. 61 (1978) 342–349.
[16] G. Bandyopadhyay, Fulrath, Processing parameters and properties of lithium ferrite spinel, J. Am. Ceram. Soc. 57 (1974) 182–186.
[17] P. Sainamthip, V.R.W. Amarakoon, Role of zinc volatilization on the microstructure development of manganese zinc ferrites, J. Am. Ceram. Soc. 71 (1988) 644–648.
[18] A.M. Sankpal, S.V. Kakatkar, N.D. Chaudhari, R.S. Patil, S.R. Sawant, Initial permeability studies on Al^{3+} and Cr^{3+} substituted Ni–Zn ferrites, J. Mater. Sci.: Materials in Electronics 9 (1998) 173–179.